

Regulated Endocytic Routing Modulates Wingless Signaling in *Drosophila* Embryos

Laurence Dubois,¹ Magalie Lecourtois,^{1,3}
Cyrille Alexandre,¹ Elisabeth Hirst,¹
and Jean-Paul Vincent^{1,2}

¹National Institute for Medical Research
The Ridgeway
Mill Hill
NW71AA London
United Kingdom

Summary

Embryos have evolved various strategies to confine the action of secreted signals. Using an HRP-Wingless fusion protein to track the fate of endocytosed Wingless, we show that degradation by targeting to lysosomes is one such strategy. Wingless protein is specifically degraded at the posterior of each stripe of *wingless* transcription, even under conditions of over-expression. If lysosomal degradation is compromised genetically or chemically, excess Wingless accumulates and ectopic signaling ensues. In the wild-type, Wingless degradation is slower at the anterior than at the posterior. This follows in part from the segmental activation of signaling by the epidermal growth factor receptor, which accelerates Wingless degradation at the posterior, thus leading to asymmetrical Wingless signaling along the anterior-posterior axis.

Introduction

Secreted signaling molecules are at the heart of metazoan pattern formation. But too much of a good thing can be deleterious and embryos have evolved various strategies to confine the activity of a signal both spatially and temporally (Freeman, 2000). Of course, transcriptional regulation of signal production and signal release from expressing cells must be important. Also relevant is the state of signal-receiving cells, such as the availability of signal transduction components or the presence of intracellular antagonists. In addition, a widespread strategy used by embryos to modulate signaling is to produce extracellular inhibitors such as Argos (Schweitzer et al., 1995a), Noggin (Zimmerman et al., 1996), or Frzb, a Wnt antagonist (Leyns et al., 1997; Wang et al., 1997). In the case of Wingless, the *Drosophila* Wnt-1 homolog, no extracellular inhibitors are known to exist and no Frzb homolog can be recognized in the genome. In the absence of extracellular inhibitors, embryos could ensure that only intended target cells activate the signaling pathway by tightly regulating posttranslationally the distribution of the signal itself. In principle, two broadly defined parameters could affect the distribution of a signal: transport and/or stability once it has reached

distant cells. In both cases, ligand availability would determine signaling intensity.

In *Drosophila* embryos, the distribution of Wingless appears to be regulated because it undergoes a transition from symmetrical to asymmetrical during stage 10, 5 hr after egg deposition (Martinez Arias, 1993; Sanson et al., 1999). Most notably, before stage 10, Wingless spreads into the *engrailed* domain (at the posterior of each stripe of *wingless* expression), while shortly thereafter, it becomes barely detectable in the same cells (Figure 1). Thus, at early stages, Wingless spreads toward the posterior to specify the width of the *engrailed* domain (an early function of Wingless) and then recedes to allow distant *engrailed*-expressing cells to acquire a denticle fate (a decision taken after stage 11) (diagram in Figure 1). How is this transition in Wingless distribution regulated and does it follow from a change in transport or stability?

Several factors could, in principle, modulate the distribution of Wingless. One likely class includes heparan sulfate proteoglycans (HSPGs), abundant cell surface molecules known to interact with Wingless. HSPGs have been suggested to sequester Wingless and thereby affect its distribution (Lin and Perrimon, 1999; Tsuda et al., 1999). A molecule from a different class, the seven-pass transmembrane receptor Frizzled2, stabilizes Wingless and thus seems to extend the Wingless gradient in *Drosophila* wing imaginal discs (Cadigan et al., 1998). Therefore, identified molecules exist that can bind to Wingless in the extracellular space. However, it is not clear how they might contribute to the asymmetry of Wingless action in embryos.

In the case of Decapentaplegic (Dpp), the *Drosophila* TGF- β homolog, recent studies have shown that endocytosis is integral to the mechanism that generates a gradient in wing imaginal discs (Entchev et al., 2000; Teleman and Cohen, 2000). Interestingly, endocytosis has been known for some time as a general strategy for signal downregulation (Ceresa and Schmid, 2000). For example, agonist-induced internalization of G protein-coupled receptors at nerve terminals limits the availability of receptors at the cell surface and thus contributes to desensitization (Tsao and Zastrow, 2000). In many instances, following internalization, the ligand is delivered to lysosomes for degradation. Thus, endocytosis could modulate the distribution of an extracellular ligand like Wingless and control its ability to signal maximally.

Here, we examine the role of endocytosis and degradation in generating the asymmetric range of Wingless in *Drosophila* embryos. To characterize Wingless trafficking through the endocytic compartment of embryonic epidermal cells, we used a horseradish peroxidase-Wingless (HRP-Wingless) fusion protein. The horseradish peroxidase (HRP) moiety of the fusion persists in degradative compartments, thus allowing us to track the fusion protein deep into the endocytic pathway and see Wingless “after it has been degraded.” With this tool, we find that cells located at the posterior of each stripe of *wingless* expression degrade Wingless more readily than at the anterior. We present functional evidence that endocyto-

²Correspondence: jp.vincent@nimr.mrc.ac.uk

³Present address: Laboratoire de Génétique Moléculaire, INSERM EPI 9906, 22 Boulevard Gambetta, 76183 Rouen, France.

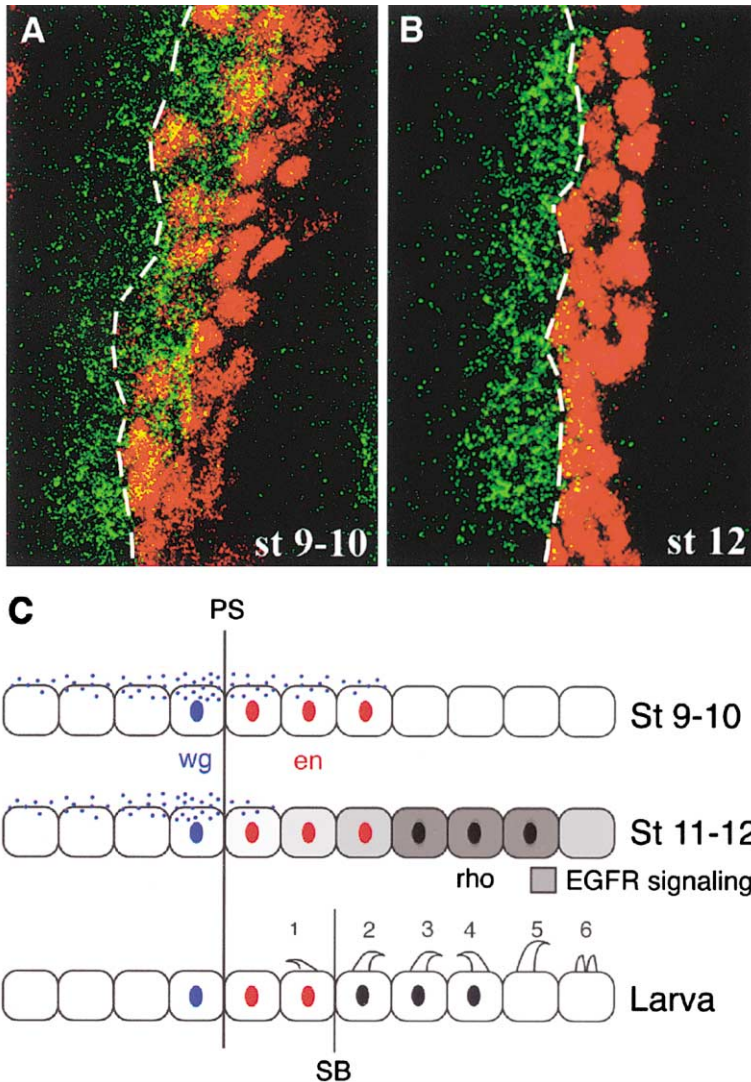


Figure 1. A Transition in the Distribution of Wingless

Top two panels show wild-type embryos stained with anti-Wingless (green) and anti-Engrailed (red) at stage 9 (A) and 11 (B). During the intervening period, Wingless-containing vesicles disappear from the domain of *engrailed* expression. This is depicted in the diagrams below (C). Until early stage 10, Wingless spreads into the *engrailed* domain and then recedes sometime during stage 10. At stage 12, Wingless-containing vesicles are infrequently detected in *engrailed*-expressing cells. At this stage, *rhomboid* begins to be expressed at the posterior of each *engrailed* stripe, leading to the activation of EGFR signaling in and around its domain of expression. The zone of Rhomboid influence corresponds roughly to where denticles form at the end of embryogenesis, while Wingless signaling is associated with the absence of denticles (bald cuticle). PS, parasegment boundary; SB, segment boundary.

sis and lysosomal degradation are required to restrict the range of Wingless at the posterior. This process is regulated in space and time by the local activation of another signaling pathway, that of the epidermal growth factor receptor (EGFR).

Results

Downregulation of the Wingless Ligand Posterior to the Source

During early *Drosophila* embryogenesis, the Wingless protein can be detected throughout the posterior compartment where it acts to sustain *engrailed* expression. Later, between stages 10 and 11, around 5 hr after egg deposition (AED), a transition occurs and Wingless becomes barely detectable within the *engrailed* domain even though it continues to be secreted by *wingless*-expressing cells (Figure 1). This early drop in Wingless staining follows from a decrease in the transcription of *frizzled* and *frizzled2* within *engrailed*-expressing cells (Lecourtois et al., 2001). Indeed, ectopic expression of *frizzled* or *frizzled2* prolongs the presence of Wingless-

containing vesicles in the *engrailed* domain (Figures 2C and 2E; also see Lecourtois et al., 2001). However, this is only a reprieve. In *engrailed-gal4 UAS-Frizzled2* or *engrailed-gal4 UAS-Frizzled* embryos, the Wingless protein still decays within the *engrailed* domain (but at a later stage, around stage 11–12; Figures 2D and 2F). This could be because transport into the *engrailed* domain is prevented or ineffective after this stage. However, the effect of a dominant-negative Frizzled2 (the N-terminal extracellular domain linked to a GPI anchor, Δ frizzled2-GPI; Cadigan et al., 1998) suggests otherwise. If Δ frizzled2-GPI is expressed in the *engrailed* domain, Wingless continues to be detected in receiving cells, even at late embryonic stages (Figures 2G and 2G'). This suggests that Wingless can be transported into the *engrailed* domain after stage 11–12. Importantly, Δ frizzled2-GPI is likely to lack an endocytic signal since it is devoid of all intracellular residues. Since expression of Δ frizzled2-GPI prevents the drop in Wingless staining within the *engrailed* domain, endocytosis of the Wingless/receptor complex could be responsible for downregulating Wingless levels (and function) there. We have

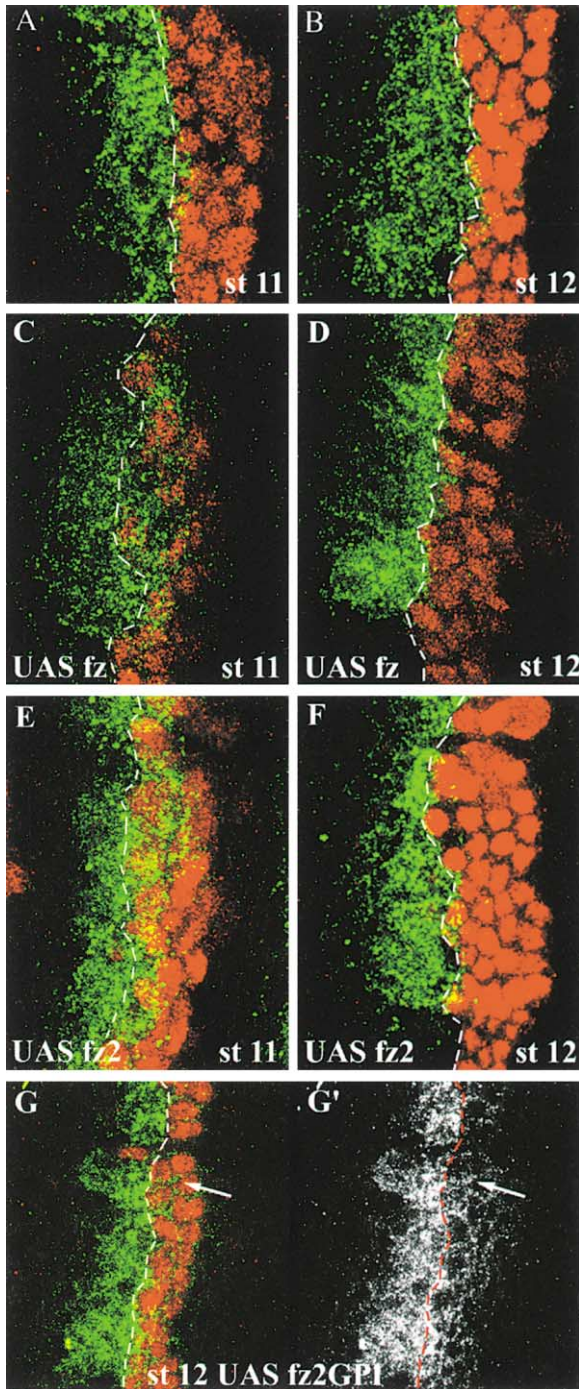


Figure 2. Stabilization of Wingless by Frizzled and Frizzled2 within the *engrailed* Domain Is Temporary

All panels show double immunofluorescence with anti-Wingless (green) and anti-Engrailed (red).

(A and B) Wild-type embryos at stage 11 (A) and 12 (B). Use these for comparison with subsequent panels. (C and D) *engrailed-gal4 UAS-Frizzled* at stage 11 (C) and 12 (D).

(E and F) *engrailed-gal4 UAS-Frizzled2* at stage 11 (E) and 12 (F). With both Frizzled and Frizzled2, Wingless is temporarily sustained but then drops.

(G and G') *engrailed-gal4 UAS-dfrizzled2-GPI* at stage 12. (G') is the same embryo as in (G), but only the Wingless staining is shown. The arrow indicates accumulation of Wingless protein posterior to the source. No drop in Wingless staining occurs within the *engrailed* domain.

explored this possibility with an HRP-Wingless fusion protein.

An Active HRP-Wingless Fusion Protein

There are two main benefits from using an HRP fusion to study endocytic trafficking. One is that HRP activity is easily detected after reaction with 3, 3' diaminobenzidine (DAB), which produces an electron-dense deposit. Unlike many antigens, HRP activity is unaffected by fixation with glutaraldehyde and therefore, ultrastructural details are optimally preserved for electron microscopy (EM). A second benefit follows from the relative stability of HRP within the destructive environment of the late endosomal and lysosomal compartments. Importantly, this appears to be true even if HRP is part of a fusion protein. As shown by Sunio et al. (1999), a Boss-HRP fusion protein is internalized by R7 cells in the fly retina (Boss is a ligand for the Sevenless receptor tyrosine kinase; Reinke and Zipursky, 1988). Anti-Boss detects the fusion only in early endosomes while anti-HRP gives staining throughout the endocytic pathway, including in lysosomes. This suggests that, as the fusion protein proceeds through the endocytic pathway, the Boss moiety is rapidly degraded while the HRP part of the fusion remains detectable even in lysosomes. Thus, tagging an endocytosed protein with HRP, enables it to "be seen," even after it has been degraded in lysosomes.

To track the degradation of Wingless in cells receiving the signal, we constructed transgenic flies expressing an HRP-Wingless fusion protein. Since modifications at the C terminus of Wingless are known to reduce signaling activity drastically (Zecca et al., 1996), HRP was inserted at the N terminus of Wingless, just downstream of the signal peptide (Figure 3A). Several genetic tests were performed to ask whether the fusion is secreted and activates the Wingless pathway. In a first test, we expressed *UAS-HRP-Wingless* ubiquitously using the *armadillo-Gal4* driver. This leads to the typical "naked" or "bald" phenotype (near absence of denticles; Lawrence et al., 1996) that characterizes an excess of Wingless signaling (Figure 3B). Note that the conversion of denticle belts to bald cuticle is not as extensive as that caused by uniform expression of *UAS-Wingless* (not shown). Thus, HRP-Wingless activates the signaling pathway but its activity is somewhat reduced compared to that of the wild-type protein. As an aside, HRP-Wingless appears to be temperature-sensitive, since more naked cuticle is induced at 18°C than at 25°C, even though the *gal4* system is less effective at lower temperature. Next, the fusion was expressed with the *wingless-gal4* driver in a *wingless* null mutant. The "lawn phenotype" (denticles everywhere; Bejsovec and Martinez Arias, 1991) that characterizes a *wingless* mutant (Figure 3C) is extensively rescued (Figure 3D) and the cuticular pattern, including the polarity and shape of individual denticles, is completely restored in many segments. In some segments, rescue is incomplete, as indicated by the fusion of denticle belts. However, incomplete rescue is also seen when *UAS-Wingless* is used in a control experiment (not shown). Most likely, in both experiments, the delay inherent to the *gal4* system contributes to the lack of full rescue. The above rescue experiment suggests that HRP-Wingless can replace endogenous

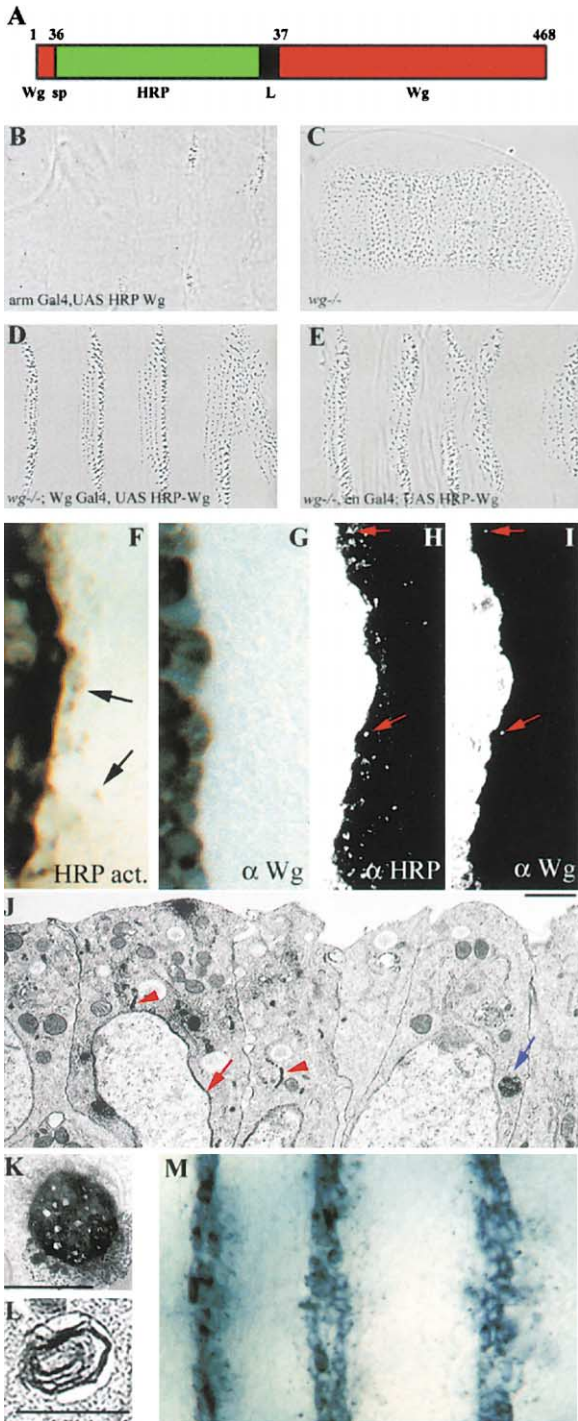


Figure 3. Activity and Localization of HRP-Wingless

(A) Schematic representation of the fusion protein. Wingless sequences are in red and HRP in green. "Wg sp" denotes the signal peptide. In black is the hinge of the λ repressor used as a linker ("L").

(B) Uniform expression of *UAS-HRP-Wingless* with the *armadillo-gal4* driver leads to suppression of denticle formation. Nearly all epidermal cells make naked cuticles. The lawn phenotype of a *wingless* mutant (shown in [C]) is rescued by the expression of *UAS-HRP-Wingless* with the *wingless-gal4* driver (shown in [D]).

(E) Larva of the genotype *engrailed-gal4 UAS-HRP-Wingless wingless⁻* show extensive rescue too.

Wingless. However, it fails to demonstrate the spread of the fusion protein in the extracellular space. This is because inheritance of Wingless within expressing cells contribute to its spread; indeed, expression of membrane-tethered Wingless also rescues *wingless* mutants substantially (Pfeiffer et al., 2000). A rescue experiment with the *engrailed-gal4* driver (which is expressed at the posterior of *wingless*) offers a more stringent test of action at a distance (Pfeiffer et al., 2000; Sanson et al., 1999). We found that driving *UAS-HRP-Wingless* with *engrailed-gal4* substantially rescues the phenotype of a *wingless* null mutant (Figure 3E). We conclude that HRP-Wingless is secreted, acts at a distance, and is sufficiently active to replace endogenous Wingless in the embryonic epidermis.

Targeting of Internalized Wingless to Degradative Structures

Having established that HRP-Wingless is active, we used it to track the fate of Wingless in cells receiving the signal. We expressed *UAS-HRP-Wingless* with *wingless-gal4* and assayed HRP activity with an in situ DAB reaction. As mentioned above, at stage 12, the Wingless protein is no longer detectable within the *engrailed* domain of wild-type embryos. By contrast, vesicles containing HRP activity are plentiful in the same cells and at the same stage in the transgenic embryos (Figure 3F). Importantly, in embryos of the same genotype, vesicles containing Wingless immunoreactivity are very rarely detected (Figure 3G), suggesting that the high number of HRP vesicles is not simply a consequence of overexpression from the *wingless-gal4* driver. Thus, it appears that, within signal-receiving cells, the Wingless moiety of the fusion is partially degraded or denatured while HRP remains. In principle, the relative excess of vesicles containing HRP activity could be due to higher sensitivity of direct DAB staining compared to immunostaining. We therefore used double immunofluorescence to detect HRP and Wingless in the same preparations of embryos expressing *UAS-HRP-Wingless* under the control of *wingless-gal4*. The two antibodies label the expres-

(F–L) Localization of HRP-Wingless in posterior nonexpressing cells of a stage 12 embryo (genotype is *wingless-gal4 UAS-HRP-Wingless*). DAB staining reveals the presence of HRP activity at the posterior of expressing cells (strongly labeled in brown) (F) while no Wingless can be detected in nonexpressing cells of embryos of the same genotype stained with anti-Wingless followed by an HRP-tagged secondary (G). (H and I) Double immunostaining of a *wingless-gal4 UAS-HRP-Wingless* embryo reveals the HRP moiety (H) and the Wingless moiety (I) of the HRP-Wingless chimera in single preparation. Arrows indicate vesicles containing both antigens. (J) Sagittal section of an embryo of the same genotype viewed by EM. Wingless-expressing cells are easily recognized by virtue of DAB staining in various organelles such as the ER (red arrowhead), and at the nuclear membrane (red arrows). Maybe the nuclear membrane stains because the fusion protein could be synthesized faster than it is secreted, resulting in transfer from the ER to the nuclear membrane. In nonexpressing cells, staining is readily seen in MVBs (blue arrow). High magnification of an MVB (K), and a lysosome (L), recognizable by its lamellar structure. (M) Whole-mount DAB of a stage 12 embryo expressing *UAS-HRP-Wingless* under the control of *engrailed-gal4*. HRP activity is clearly seen on either side of the expression domain, especially at the posterior. Scale bars: 1 μ m (J), 0.5 μ m (K and L).

sion domain with comparable intensity, suggesting that they have similar affinity for their respective epitope. Nevertheless, in posterior signal-receiving cells, there is a clear difference between the two channels. While very few vesicles contain both the Wingless and HRP antigens, many vesicles are positive only with the anti-HRP antibody (compare Figure 3H [HRP] with 3I [Wingless]). Thus, within cells receiving the signal, the Wingless moiety of the fusion protein disappears quickly relative to the HRP portion. This suggests that the fusion protein is targeted to the lysosomal compartment where only HRP would be detectable.

To confirm that much of the HRP activity detected in the above experiment is in degradative structure, embryos expressing HRP-Wingless were analyzed by EM. For such analysis, it is crucial to distinguish cells receiving the signal from those expressing it. Expressing cells are easily recognizable because their Golgi apparatus and endoplasmic reticulum and even the nuclear membrane are heavily labeled with DAB deposits (Figure 3J). Staining in all these structures was used to recognize expressing cells. The subcellular location of HRP was then assessed in posterior, nonexpressing cells. There, HRP activity is mainly localized within degradative structures such as multivesicular bodies (MVBs, already observed by Gonzalez et al., 1991 and van den Heuvel et al., 1989) (Figure 3K) and lysosomes (Figure 3L). We conclude that, at stage 12, HRP-Wingless is rapidly endocytosed and targeted to lysosomes in cells posterior to the normal domain of *wingless* expression. Presumably, in the wild-type, Wingless is barely detectable in the same region because targeting to lysosomes is so rapid.

As we showed previously, overexpression of Wingless in the *engrailed* domain has relatively minor phenotypic consequences (Sanson et al., 1999). In particular, no bald cuticle is induced at the posterior of the source, suggesting a failure of Wingless to act in this direction. Indeed, in stage 12 *engrailed-gal4 UAS-Wingless* embryos, very little Wingless protein is detected at the posterior of *engrailed* cells, despite their massive overexpression of Wingless. This could be due to a block of Wingless transport across the segment boundary at the posterior of the *engrailed* domain. However, the above results suggest an alternative, namely that Wingless is transported toward the posterior but is rapidly degraded there and therefore undetectable. We tested this possibility by expressing *UAS-HRP-Wingless* with *engrailed-gal4*. Many HRP-containing vesicles can be seen at the posterior even at stages 12–13 (Figure 3M). As shown in the next section, for the most part, these vesicles are degradative structures (recognized by EM) and do not contain Wingless immunoreactivity. Thus the HRP-Wingless fusion (and presumably Wingless too) does cross the segment boundary toward the posterior but is rapidly forwarded to lysosomes. Taken together, the above results show that the zone of Wingless degradation includes the *engrailed* domain and more posterior cells.

Differential Rates of Lysosomal Targeting along the Anterior-Posterior Axis

The range of Wingless action is asymmetric in the embryonic epidermis (Sanson et al., 1999). This is best

shown in *wingless* mutant embryos that express Wingless in the *engrailed* domain because, after stage 11, the *engrailed* domain has well-defined boundaries both at the anterior and the posterior; hence, we can compare the fate of endocytic Wingless on both sides of the source. In such embryos (whose only source of Wingless is the *engrailed* domain), naked cuticle is made over 3–4 cell diameters at the anterior while no naked cuticle is made at the posterior. We now ask if this asymmetry is correlated with differential lysosomal targeting. We expressed *UAS-HRP-Wingless* with *engrailed-gal4* and used EM to identify HRP-containing vesicles in nonexpressing cells on both sides of the source. Labeled (HRP-containing) degradative structures are particularly easy to recognize because they are large. These were counted over a range of three cells on either side of the expression domain. Data was collected from several sections of stage 12 embryos (Figure 4A and Experimental Procedures). As expected, more vesicles are detected, on average, near the source. Superimposed on this graded distribution, a clear difference can be seen between anterior and posterior. Overall, we found four times more labeled MVBs and lysosomes at the posterior than at the anterior (Figure 4B). Thus, HRP-Wingless is preferentially targeted to degradative structures at the posterior. We cannot formally distinguish whether increased degradation follows from increased endocytosis or increased targeting of endocytic vesicles to degradative structures.

As argued above, a vesicle that contains both HRP and Wingless immunoreactivity is presumed to be an early endosome while, if only HRP is detectable, it is likely to be at a later stage of the endocytic pathway. Using double immunofluorescence, we find many vesicles containing both Wingless and HRP at the anterior of the expression domain. By contrast, most vesicles at the posterior are only stained with anti-HRP, confirming that they are degradative structures. (compare Figures 4C and 4D). We suggest that, in posterior cells, Wingless is actively targeted to the lysosomal compartment while at the anterior, internalized Wingless lingers in early endosomes or is recycled (although some degradation takes place, too). Note that although confocal microscopy clearly reveals vesicles that contain HRP (and Wingless) at the anterior, such vesicles cannot be unambiguously identified by EM. Maybe they are too small or they contain too little fusion protein for the DAB reaction to generate enough contrast.

Downregulation of Wingless Signaling at the Posterior Requires Rapid Degradation

So far, we have shown a clear inverse correlation between the rate of targeting to lysosomes and the ability of Wingless to signal. We now ask if compromising lysosomal targeting affects signaling output. The endocytic pathway is affected by mutations in a variety of genes. One is *clathrin*, a gene required for endocytosis (Bazin et al., 1993). Another is *deep orange*, which encodes a homolog of the yeast vacuolar protein-sorting protein, Vps18p. In *Drosophila*, the *deep orange* gene product is required for normal delivery of proteins to lysosomes (Sevrioukov et al., 1999). Unfortunately, one cannot generate embryos lacking the function of either gene be-

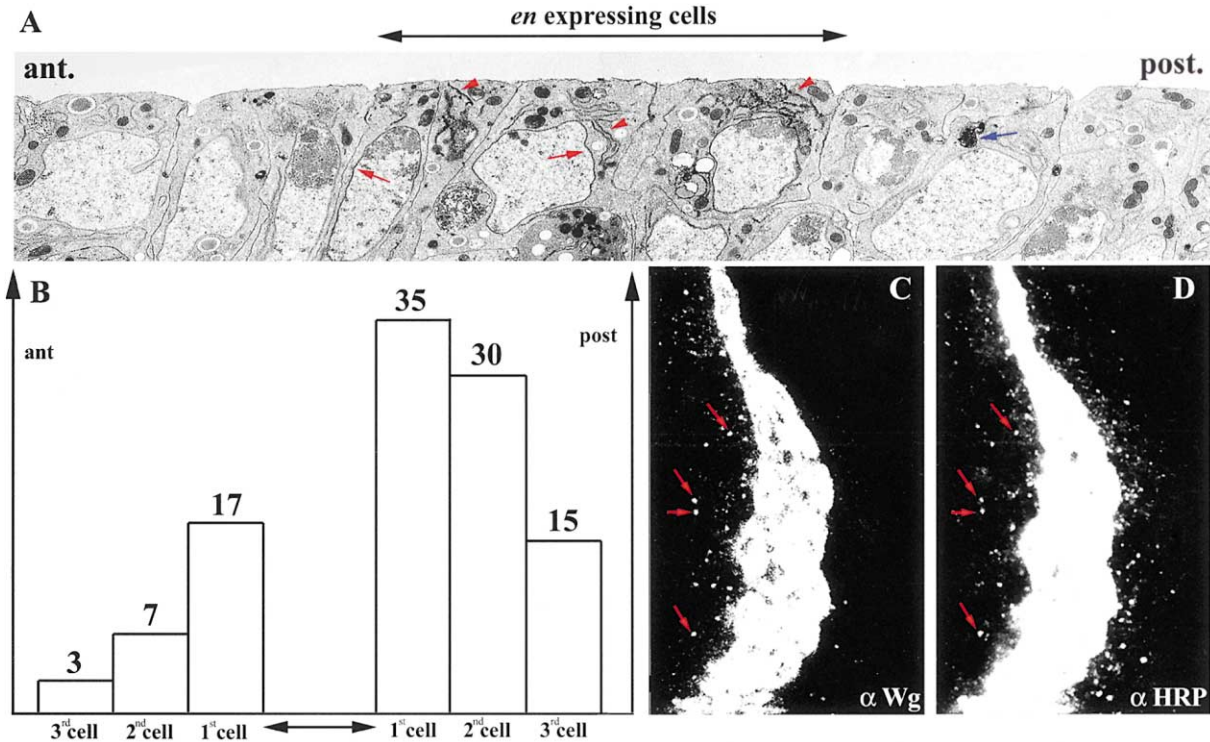


Figure 4. HRP-Wingless Is Preferentially Targeted to Lysosomes at the Posterior

In all panels, HRP-Wingless is expressed under the control of the *engrailed-gal4* driver.

(A) Sagittal section of the epidermis at stage 12 showing expressing and nonexpressing cells. Two-headed arrow indicates the domain of expression as identified by stained nuclear membrane (red arrows) and ER (red arrowheads). The blue arrow indicates an MVB in a nonexpressing cell. Ant, anterior; Post, posterior.

(B) In 35 such sections, MVBs and lysosomes were counted over three cell diameters on either side of the expression domain and data was plotted on a histogram. Like in (A) the double arrow represents the expressing domain.

(C and D) Double immunostaining with anti-Wingless (C) and anti-HRP (D). Arrows point to vesicles where both parts of the fusion protein are detectable. These are mostly seen at the anterior (rarely at the posterior) and are presumed to represent early or recycling endosomes. Scale bar: 1 μ m.

cause both genes have a strong maternal contribution that is required for oogenesis. Zygotic mutants of *clathrin* or *deep orange* proceed through development relatively normally and die only at the end of embryogenesis, without an obvious phenotype. In particular, the denticle pattern is essentially normal. We reasoned that such zygotic mutants would have reduced activity of the corresponding gene (since they only have maternal products) and may therefore show a phenotype in a sensitized genetic background. As mentioned above, overexpression of Wingless with the *engrailed-gal4* driver leads to a relatively mild phenotype (in particular, row 2 denticles are present even though they are adjacent to the Wingless-misexpressing cells; Figures 5A and 5B). Presumably, the degradation machinery acting at the posterior is able to cope with the excess Wingless. However, this is no longer the case when the activity of *clathrin* or *deep orange* is reduced. In the absence of zygotic contribution from *clathrin* or *deep orange*, Wingless originating from the *engrailed* domain produces excess naked cuticle within areas normally occupied by denticle belts (Figures 5C and 5D, respectively), an indication of excess Wingless signaling at the time when cuticular fates are specified.

The above result suggests that in *clathrin* or *deep*

orange mutants, excess Wingless is no longer degraded fast enough to allow denticle formation. This was confirmed by looking directly at Wingless protein in embryos that lack the zygotic contribution of *clathrin* or *deep orange* and express *wingless* under the control of *engrailed-gal4* (Figures 5E–5H). As controls, we used embryos that express Wingless with *engrailed-gal4* but are otherwise wild-type. Controls were imaged at the same settings as the mutants to allow a comparison between staining intensities. In either mutant, increased Wingless staining is seen both anterior and posterior to the source (compare Figure 5E with 5F and Figure 5G with 5H). In *deep orange* mutants, Wingless seems to accumulate in intracellular vesicles, some of which appear enormous (arrow in Figure 5F). These are likely to be similar to the giant MVBs reported to accumulate in photoreceptors of *deep orange* animals (Sevrioukov et al., 1999). Note that in *deep orange* mutant embryos, staining is also strongly increased within the domain of expression. Most likely, expressing cells continue to endocytose Wingless at a high rate but cannot forward it to late endosomal compartments. In *clathrin* mutants, excess Wingless appears to localize at the cell membrane (Figure 5H), consistent with the role of *clathrin* in endocytosis.

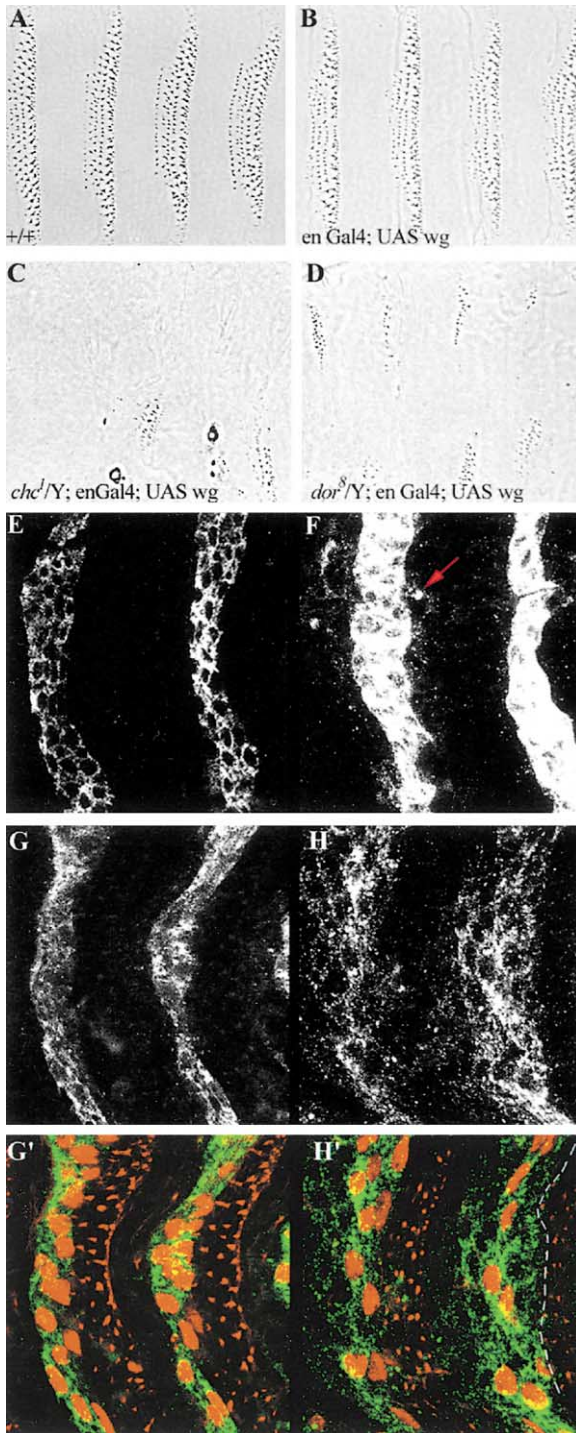


Figure 5. *clathrin* and *deep orange* Are Required for the Removal of Excess Wingless

(A–D) Ventral cuticle of first instar larvae. (A) Wild-type. (B) *engrailed-gal4 UAS nuclacZ; UAS-Wingless*. Note that the only apparent phenotype is a loss of row 1 denticle. (C) Same genotype as in (B) except also *clathrin* mutant (*chc¹/Y; engrailed-gal4 UAS nuclacZ; UAS-Wingless*). (D) Same genotype as in (B) except also *dor* mutant (*dor⁸/Y; engrailed-gal4 UAS nuclacZ; UAS-Wingless*). Note the excess naked cuticle in both (C) and (D) compared to (B). Neither mutation on its own has a noticeable effect on the cuticle pattern. (E) Wingless protein distribution in a stage 14 *engrailed-gal4 UAS nuclacZ; UAS-Wingless* embryo (same genotype as in [B]).

In *clathrin* mutants, the spread of Wingless appears to broaden (Figure 5H), in apparent contradiction with the report that a mutation in *shibire* (which encodes Dynamin) reduces the range of Wingless in *Drosophila* embryos (Bejsovec and Wieschaus, 1995). In fact, Bejsovec and colleagues (e.g., Moline et al., 1999) have suggested that recycling of internalized Wingless powers transport of the signal by a mechanism of planar transcytosis. However, Strigini and Cohen (2000) have shown that, in imaginal discs, *shibire* is required for both endocytosis and secretion. Therefore, the apparent reduction in the spread of Wingless in *shibire* mutant embryos could be due to reduced secretion. Clearly, the role of endocytosis (and planar transcytosis) in Wingless transport along the embryonic epidermis must be reexamined.

As can be seen in Figure 5, loss of *clathrin* or *deep orange* function leads to the accumulation of Wingless at the anterior (as well as the posterior) of the source. This suggests that Wingless is also degraded at the anterior. We propose that the difference between anterior and posterior cells is quantitative. Indeed, our EM analysis shows that Wingless is targeted to lysosomes at the anterior but less frequently than at the posterior.

Denticles are synthesized on a template of actin protrusions that form around stage 15. Therefore, the prospective denticle pattern can be recognized before cuticle deposition by staining with phalloidin (Dickinson and Thatcher, 1997). The embryo shown in Figure 5H' was fixed late enough that the actin bundles had already formed. As can be seen, the area where Wingless accumulates correlates with the absence of actin bundles (outlined by the dotted line in Figure 5H'). This confirms the functional link between lack of Wingless degradation and the formation of naked cuticle.

Chloroquine Causes Excess Wingless Signaling

Clearly, *clathrin* and *deep orange* are needed to remove excess Wingless signal. We now ask if lysosomal degradation of Wingless is needed when normal quantities of

(F) Same genotype as in (E) except also *dor⁸/Y*; (E) and (F) were stained with anti-Wingless and imaged under identical conditions. Note the increased signal in both expressing and nonexpressing cells. Also notable are the large intracellular vesicles that can be seen in signal-receiving cells (red arrow).

(G) Same as in (E) but older embryo (stage 15). This is a control for the effect of *chc* mutation shown in (H).

(H) *chc¹/Y; engrailed-gal4 UAS nuclacZ; UAS-Wingless* (same genotype as in [C]) stained with anti-Wingless and imaged under the same conditions as in (G). Note the increased and broader staining that appears to outline cells.

(G' and H') Identical frames as in (G) and (H), respectively, but with more channels shown ([G'] is control; [H'] is *chc¹/Y*). Anti- β -galactosidase and phalloidin are both shown in red and anti-Wingless in green. Phalloidin staining reveals prospective denticle belts and is easily distinguished from β -galactosidase staining, which is nuclear (and marks *engrailed*-expressing cells). The dotted line in (H') outlines a region where excess Wingless (green) could not be disposed of. Phalloidin staining (red) is suppressed in this area. Note that endogenous Wingless is not seen in the control embryos. This is because expression is reduced at the late stages shown (14–15) and also because the sensitivity of detection was intentionally set low to allow comparison with the mutants, which stain more strongly.

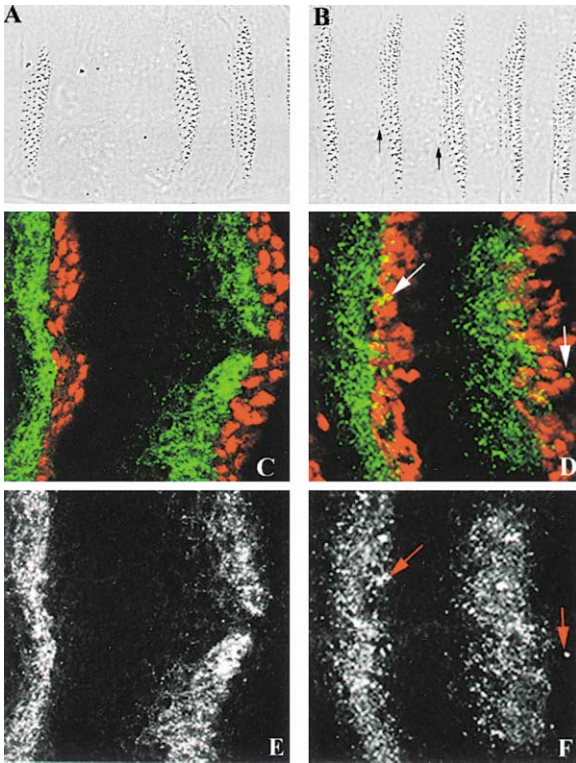


Figure 6. Lysosomal Function Is Needed to Downregulate Wingless Signaling in Wild-Type Embryos

(A and B) Two examples of cuticle pattern made by larvae derived from embryos injected at stage 9 with chloroquine into the perivitelline space. Note the missing denticle belt in (A). Arrows in (B) point to missing row 1 denticles (compare with wild-type in Figure 5A). (C and D) Double immunolabeling with anti-Wingless (green) and anti-Engrailed (red). (C) Stage 12 embryo whose perivitelline space was injected with buffer at stage 9 (control). (D) Stage 12 embryo whose perivitelline space was injected with chloroquine at stage 9. (E and F) show the same frames as (C) and (D), respectively, but only Wingless staining is shown. Arrows in (F) point to large Wingless-containing vesicles that are seen in chloroquine-injected embryos but never in control embryos.

Wingless are produced, such as in a wild-type embryo. As stated above, mutations in *clathrin* or *deep orange* are either too strong to permit cell viability or too weak to show a recognizable phenotype in embryogenesis. Using chloroquine, an antimalarial drug, we were able to inhibit lysosomal function in a subtler manner. Chloroquine is not membrane permeant and reaches late endosomal compartments through the endocytic pathway. There, it raises the pH and thus interferes with normal function (Kurz et al., 2000). In order to preferentially block lysosomal function in epidermal cells, we injected chloroquine (100 mg/ml) into the perivitelline space around stage 9–10 ($n = 165$). As a control, buffer was injected in the perivitelline space ($n = 104$). Sixteen percent of the chloroquine-injected embryos went on to form large patches of ectopic naked cuticle (Figure 6A). By comparison, ectopic naked cuticle was rarely seen in control embryos (3%) and covered much smaller areas. In a further 27% of chloroquine-injected embryos, row 1 denticles were lost in one or more segment (Figure 6B). This was seen in only 3% of the control, buffer-

injected, embryos. Overall then, excess naked cuticle was seen in 43% of the chloroquine-injected embryos, compared to 6% in the controls. This phenotype is most likely due to excess Wingless signaling following a failure to degrade endogenously produced Wingless at the time when Wingless is normally degraded to allow the specification of denticle fates. Indeed, many Wingless-containing vesicles were detected in the *engrailed* domain of chloroquine-injected embryos, even as late as stage 12 (Figure 6D), whereas, in the controls, very few such vesicles are seen (Figure 6C). As seen in Figure 6, chloroquine not only affects the overall distribution of Wingless but also its subcellular localization. Large Wingless-containing vesicles are seen (arrow in Figure 6F), an observation that is consistent with a block of lysosomal degradation and the accumulation of Wingless in an endosomal compartment. In conclusion then, downregulation of the Wingless protein is required to terminate signaling and ensure that no ectopic naked cuticle forms.

Genetic Control of Wingless Degradation

The spatial and temporal regulation of Wingless degradation implies the existence of one or several regulatory genes that are activated at the posterior and not at the anterior of each *wingless* stripe. As we have shown previously (Sanson et al., 1999), the activity of *hedgehog*, as well as that of its downstream effector *cubitus interruptus*, are needed to prevent the spread of Wingless toward the posterior. In *hedgehog* (or *cubitus interruptus*), mutant embryos that overexpress *wingless* under the control of *engrailed-gal4*, many Wingless-containing vesicles are detected at the posterior and this correlates with increased Wingless signaling there. In light of our present results, we presume that a target of *hedgehog* is needed to accelerate Wingless degradation at the posterior. One candidate target gene is *rhomboid*, because it is only expressed at the posterior of each stripe of *engrailed* (and *hedgehog*) expression (Alexandre et al., 1999). Moreover, segmental expression of *rhomboid* commences around stage 11, roughly the stage when the second phase of Wingless degradation begins. By analogy with the experiments with *hedgehog* and *cubitus interruptus*, we looked at *rhomboid* mutants that overexpress Wingless under the control of *engrailed-gal4* and found increased Wingless staining both within and at the posterior of each *engrailed* stripe (Figures 7A and 7B). Thus, in the absence of *rhomboid*, Wingless degradation is impaired. This result implicates EGFR signaling, since *rhomboid* encodes a limiting factor needed for the activation of the EGFR ligand Spitz (Schweitzer et al., 1995b). A null mutation in EGFR leads to extensive morphological defects, thus making staging and analysis difficult (Clifford and Schupbach, 1992). Nevertheless, in embryos that we could analyze (of the genotype *engrailed-gal4 UAS-Wingless EGFR⁻*), excess Wingless is detected at the posterior of the expression domain (Figure 7C). The role of EGFR could be mediated by a target gene of the MAP kinase pathway. Alternatively, or in addition, a nontranscriptional response to EGFR signaling could lead to Wingless degradation. We looked at the role of Pointed, a transcription factor that mediates many activities of the EGFR in *Drosophila* (Ga-

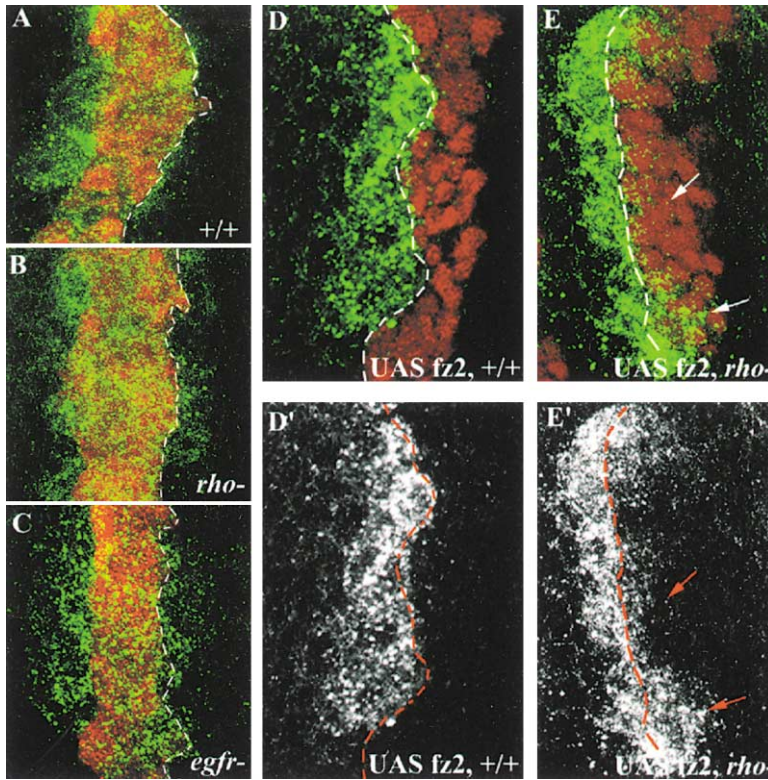


Figure 7. EGFR Signaling Modulates the Rate of Wingless Degradation

(A) Double immunostaining with anti-Wingless (green) and anti- β -galactosidase (red) of *engrailed-Gal4 UAS-Wingless UAS-LacZ* at stage 12. Few Wingless vesicles are detected posterior to the *engrailed* domain (recognized by β -galactosidase staining). Note that endogenous Wingless expression contributes to signal at the anterior.

(B and C) Same staining of stage 12 embryos of the same genotype except also *rhomboid* mutant (B) or *egfr* mutant (C). Relatively many more Wingless-containing vesicles are seen at the posterior.

(D) Double immunostaining with anti-Wingless (green) or anti-Engrailed (red) of a stage 12 embryo carrying *engrailed-Gal4 UAS-Frizzled2*. At this stage, the Wingless-containing vesicles that previously accumulated in the *engrailed* domain (shown in Figure 2E) have been eliminated (as shown in Figure 2F).

(E) Same staining of a stage 12 embryo of the same genotype except also *rhomboid* mutant. Many more Wingless-containing vesicles are detected within the *engrailed* domain.

(D' and E') same as (D) and (E) but only the Wingless staining is shown. The arrows in (E) and (E') point to "ectopic" Wingless-containing vesicles. In all panels, the dotted line marks the posterior edge of the *engrailed* domain.

bay et al., 1996; Wasylyk et al., 1997). In embryos of the genotype *engrailed-gal4 UAS-Wingless pointed⁻*, excess Wingless accumulates posterior to the source (not shown). Therefore, it appears that a transcriptional target of EGFR signaling is involved in modulating Wingless degradation.

Next, we used *rhomboid* mutants to assess the role of EGFR signaling when wild-type levels of Wingless are produced. This cannot be done by simply looking at *rhomboid* mutants because the first phase of Wingless clearance (following transcriptional repression of *frizzled* and *frizzled2*) already brings Wingless below detection level. Receptor expression was therefore artificially maintained in *rhomboid* mutants (*engrailed-gal4 UAS-Frizzled2 rhomboid⁻*). The general morphology of such embryos is again somewhat aberrant. Nevertheless, we could clearly see that Wingless-containing vesicles linger within the *engrailed* domain, even as late as stage 12, thus confirming the role of *rhomboid* in targeting Wingless to lysosomes (Figures 7D and 7E, and 7D' and 7E'). Although this is hard to prove formally, Wingless accumulation in *rhomboid* mutants appears to be in intracellular vesicles (arrows in Figure 7E'). In particular, the subcellular distribution of Wingless is clearly different from that seen in *clathrin* mutants (Figure 5H) or in embryos expressing Δ frizzled2-GPI (Figure 2G'); two situations when Wingless accumulates at the cell surface. In conclusion, we suggest that Rhomboid (and EGFR) regulates the transfer of Wingless from endosomes to degradative structures. However, it is unlikely to be the sole regulator since not all *engrailed*-expressing cells accumulate Wingless in the *rhomboid* mutant. Additional regulators might include a redundant homo-

log of *rhomboid* (Wasserman et al., 2000) or a gene controlling a parallel degradation pathway.

Discussion

Lysosomal Targeting Is Segmentally Modulated and Makes the Range of Wingless Asymmetric

Starting around stage 10, the range of Wingless becomes asymmetric within the embryonic epidermis of *Drosophila*. At this stage, Wingless protein disappears from the cells that are located immediately posterior to the source. Clearance of Wingless occurs in two temporally distinct phases. A first phase results from a decrease in the transcription of *frizzled* and *frizzled2* (even though residual expression remains; Lecourtois et al., 2001). Presumably, sustained levels of either receptor at the cell surface protects Wingless from degradation by extracellular proteases (Cadigan et al., 1998). However, even in the presence of higher than basal receptor expression, Wingless protein still disappears from posterior cells, although with a delay. Using an HRP-Wingless fusion protein, we have shown that this second mode of Wingless degradation involves the targeting of Wingless to lysosomes. Although we have not yet proven this formally, we suspect that endocytosis of Wingless is receptor-mediated because a Frizzled2 receptor lacking all intracellular residues binds Wingless but does not cause internalization. The outcome of either treating embryos with chloroquine (an inhibitor of lysosomal function) or reducing the activity of *clathrin* or *deep orange* shows that endocytosis and subsequent forwarding to lysosomes is needed to remove excess Wingless and downregulate signaling. We suspect that

if specific mutations of *frizzled* or *frizzled2* affecting internalization, but not signaling, could be obtained (e.g., by mutating the endocytic dileucine motif [Kirchhausen, 1999] that we noticed in Frizzled2), they would also lead to excess signaling.

Targeting of embryonic signals to lysosomes is likely to be a general strategy to restrict the range of action of morphogens and downregulate signaling. In chick embryos, Sonic Hedgehog is internalized by its receptor Patched-1 and subsequently transferred to lysosomes (Incardona et al., 2000). Likewise in *Drosophila* imaginal discs, the Hedgehog/Patched complex is quickly internalized, although the ultimate destination has not been identified (Denef et al., 2000). For Decapentaplegic, it is now clear that the right balance between recycling and degradation is needed to generate a gradient in imaginal discs (Entchev et al., 2000). The above examples show the importance of endocytic trafficking in regulating the distribution of a secreted signal (and possibly its ability to signal) but as yet, spatial regulatory control has not been demonstrated. As we have shown, degradation of Wingless is specifically accelerated over a broad area located at the posterior of each stripe of *wingless* expression (including the *engrailed*-expressing and more posterior cells). This is specific to Wingless because Hedgehog signaling continues on both sides of the *engrailed* domain throughout development. Our work therefore uncovers the spatially regulated degradation of a specific signal.

Regulation of Trafficking and Signaling

In mammalian cells, components of the EGFR signaling machinery are internalized along with the ligand/receptor complex (Bergeron et al., 1995), suggesting that signaling could persist after endocytosis. Consistent with the notion that Wingless continues to signal after internalization (but before degradation), excess signaling correlates with the accumulation of intracellular Wingless-containing vesicles in *deep orange*, *rhomboid*, and chloroquine-injected embryos. However, endocytosis is not necessarily required for signaling since loss of *clathrin* activity leads to excess Wingless signaling. Overall, existing experimental results suggest that targeting to lysosomes must follow endocytosis for downregulation of the signal. In the case of the mammalian EGFR, a specific posttranslational modification of the receptor appears to regulate endocytosis and signaling while endosome-to-lysosome transfer may occur by default (Carpenter, 2000). Because Wingless appears to accumulate in intracellular vesicles in *rhomboid* mutants, we suggest that, by contrast, endocytosis of the Frizzled/Wingless complex may occur by default while regulation takes place at a subsequent routing step. What is the nature of the regulatory control and where does it impinge on the endocytic pathway remain largely unknown, although, as we describe below, there are leads to follow.

In established examples of receptor desensitization by endocytic targeting (e.g., the mammalian EGFR or the β -adrenergic receptor), degradation is induced by ligand binding (Bohm et al., 1997; Carpenter, 2000). In contrast, Wingless degradation does not appear to be self-induced. Instead, a distinct signaling pathway is

implicated. As we have shown, *rhomboid*, a gene involved in the activation of the EGFR ligand Spitz, is required. Moreover, degradation occurs roughly in the cells where EGFR signaling is active (*rhomboid* expressing and flanking cells; see Figure 1). Because *rhomboid* is expressed at the posterior of each *engrailed* stripe, degradation is unilateral and thus leads to asymmetric Wingless action in the embryonic epidermis. Our favored model is that, once endocytosed, Wingless can either be recycled to the cell surface or forwarded for degradation, and that EGFR signaling accelerates the lysosomal transfer of vesicles fated for degradation. The requirement of *pointed* suggests that a transcriptional target of EGFR signaling is involved, although upstream phosphorylation events associated with the MAP kinase pathway could also contribute. In any case, we expect that activation of the EGFR leads to posttranslational modification (such as phosphorylation or ubiquitination; Levkowitz et al., 1999) of intracellular residues within Frizzled and Frizzled2.

Is Wingless trafficking similarly regulated in other parts of the fly? In wing imaginal discs, overexpression of *frizzled2* around the prospective wing margin (a source of Wingless) leads to the persistent stabilization of Wingless (Cadigan et al., 1998). No subsequent clearance by targeting to lysosomes seems to take place and Wingless action is indeed symmetrical in this system. Therefore, lysosomal targeting (or rather accelerated lysosomal targeting) is not a default pathway. At a different location of the wing disc, at the edge of the wing pouch, a sharp drop in Wingless staining has been noticed (Cadigan et al., 1998). Our HRP-Wingless may help test whether this corresponds to an area of rapid degradation. Note that the role of EGFR signaling may be specific to embryos since EGFR is not activated at the edge of the wing pouch. There, expression of our hypothetical EGFR target would be activated by other means.

Pattern Formation and the Spatiotemporal Control of Wingless Signaling

Previous work has shown that EGFR signaling activates *shavenbaby*, a gene that is repressed by Wingless signaling and contributes to denticle formation (Payre et al., 1999). In this instance, antagonism between the two signals is believed to occur at the level of DNA. Thus, two distinct mechanisms ensure that no Wingless signaling can occur within the zone of active EGFR signaling. Since both mechanisms depend on *rhomboid* expression, the action of Wingless begins to be curbed around stage 11, when segmental expression of *rhomboid* begins. This temporal regulation of Wingless is necessary because signaling requirements change over time. During early development, Wingless needs to act posteriorly over several cell diameters to maintain *engrailed* expression. At later stages, only a subset of *engrailed* cells (those nearest to the source) are destined to make bald cuticle and therefore require the Wingless signal. More posterior cells (including both *engrailed* expressing and nonexpressing cells) are fated to secrete denticles, a fate that is incompatible with Wingless signaling. Therefore, the most posterior *engrailed*-expressing cells need Wingless early but not late when cuticular fates are specified, hence the delayed antagonism of

Wingless signaling. Note that *engrailed* expression is not affected by Wingless downregulation because it becomes *wingless*-independent around stage 11.

Interestingly, Wingless signaling represses the transcription of *rhomboid* (Alexandre et al., 1999). Mutual antagonism between Wingless and EGFR may contribute to the establishment of a sharp boundary of gene expression where the segment border forms. Since Wingless is a positive regulator of *engrailed* expression and a negative regulator of *rhomboid* expression, the limit of the range of Wingless at early stage 11 marks the interface between *engrailed* and *rhomboid* expression (Alexandre et al., 1999). Once delineated, this interface could not become blurred because any Wingless that might spread subsequently is degraded, and thus unable to repress *rhomboid* expression. Thus, the position of a developmental boundary is locked into place by a negative feedback loop between two signaling pathways.

Experimental Procedures

Drosophila Stocks

wg^{CX4}, *dor⁸*, *chc¹*, *rhom^{7M42}*, *rhom^{PΔ5}*, *egfr¹*, are presumed null alleles (see flybase at <http://gin.ebi.ac.uk:7081/>). The following transgenic stocks were used: *engrailed*-Gal4 and UAS-*LacZ* (gift from A. Brand, Wellcome Institute, Cambridge, UK), *armadillo*-Gal4 (Sansom et al., 1996), *wingless*-Gal4 (J. Pradel, CNRS Marseilles, France), *wingless*-Gal4 (Pfeiffer et al., 2000), UAS-*frizzled* and UAS-*Frizzled2* (Zhang and Carthew, 1998), UAS-*Δfrizzled2-GPI* (Cadigan et al., 1998), UAS-*Nuc-LacZ* (M. Muskavitch, Indiana University), and UAS-*Wingless* (Lawrence et al., 1996). To make UAS-*HRP-Wingless*, DNA encoding HRP (Connolly et al., 1994) was inserted into a *wingless* cDNA using standard PCR-based cloning. The insertion site was just downstream of the DNA encoding the signal sequence, after Met 37. The 3' end of the HRP fragment was separated from the bulk of *wingless* by 139bp encoding the hinge region of the C1 lambda repressor (thus providing a flexible link between the two halves of the chimera; Astromoff and Ptashne, 1995). The relevant sequence of the resulting fusion protein was: **MET (37) Trp Gly [Gln (2) . . . Ser (309)] Ser Leu Trp Trp Val (90) . . . Ser (132) Leu TRP (38)**, where the amino acids from HRP are bracketed, the extra amino acids created by the fusion are in *italic*, the amino acids from the C1 lambda repressor are underlined, and the amino acids from Wingless are in **bold**. Numbers in parentheses indicate the position of residues within their native protein. DNA encoding the HRP-Wingless fusion protein was then cloned in pUAST and the construct was introduced in *w¹¹¹⁸* hosts by P element-mediated transformation using standard methods.

Embryo and Cuticle Preparations

Immunofluorescence was done according to standard protocols (Vincent and O'Farrell, 1992) using AlexaTM fluorescent conjugates (AlexaTM 488 and AlexaTM 592, Molecular Probes). Antibodies used were: rabbit anti-*Engrailed* (gift from C.H. Girdham and P. O'Farrell, UCSF), mouse anti-Wingless (4D4) from the Developmental Studies Hybridoma Bank, goat anti-HRP (Sigma), and rabbit anti-β-galactosidase (Cappel). For staining with Phalloidin Texas red (Molecular Probes), embryos were manually devitelinized to avoid methanol treatment, which destabilizes the cytoskeleton. Immunofluorescent staining of injected embryos was done as described in Vincent and O'Farrell, (1992). Embryos expressing HRP-Wingless were incubated at 18°C to maximize activity; all other experiments were done at 25°C.

For visualization of the cuticle pattern, 24-hour-old embryos were mounted in Hoyer's and photographed in DIC or phase contrast microscopy.

Electron Microscopy

To visualize the HRP-Wingless chimera by EM, embryos were fixed 10 min in heptane saturated with glutaraldehyde and then deviteli-

nized by hand in PBS. We found that glutaraldehyde fixation preserves HRP activity, while standard fixatives for immunostaining, which contain formaldehyde, strongly reduce the HRP activity of the fusion. Fixed embryos were transferred in 0.1 M Tris-HCL (pH 7.5) and 0.15 M NaCl, for 10 min. The TSATM Biotin system (NEN) and the ABC kit (Vector) were used in sequence to amplify the HRP signal. HRP activity was eventually revealed by incubation in DAB (0.5 mg/ml) + 0.003% H₂O₂ for 30 min. Embryos were then washed in PBS and processed for EM.

For EM, embryos were embedded as described by Van Vactor et al. (1991). Sections (70–80 nm) were poststained in Reynold's lead citrate and examined with a Jeol transmission electron microscope (Jeol CX100). We counted MVBs and lysosomes in 35 sections taken from a total of 4 embryos. When considering a given embryo, only sections separated by at least 3–4 μm were analyzed to ensure that no vesicle be counted twice.

Chloroquine Injections

A solution of chloroquine (Sigma; 100 mg/ml in 10% PBS) was injected in the peri-vitelline space at stage 9–10. Control embryos were injected at the same stage with 10% PBS only. Injection was done according to standard protocols. After injection, embryos were incubated at 25°C until they reached the desired stage.

Acknowledgments

We thank James Briscoe, Jose Casal, and Peter Lawrence for comments on the manuscript; Helmut Kramer for advice; Ian Burdett for discussions; the Developmental Studies Hybridoma Bank and Steve Cohen for antibodies; and the Bloomington Stock Center for *Drosophila* stocks. M.L. was supported by an EMBO postdoctoral fellowship. L.D. was supported in part by the Association pour la Recherche contre le Cancer. All other support came from the United Kingdom's Medical Research Council.

Received March 21, 2001; revised May 9, 2001.

References

- Alexandre, C., Lecourtois, M., and Vincent, J. (1999). Wingless and Hedgehog pattern *Drosophila* denticle belts by regulating the production of short-range signals. *Development* 126, 5689–5698.
- Astromoff, A., and Ptashne, M. (1995). A variant of lambda repressor with an altered pattern of cooperative binding to DNA sites. *Proc. Natl. Acad. Sci. USA* 92, 8110–8114.
- Bazinet, C., Katzen, A.L., Morgan, M., Mahowald, A.P., and Lemmon, S.K. (1993). The *Drosophila* clathrin heavy chain gene: *clathrin* function is essential in a multicellular organism. *Genetics* 134, 1119–1134.
- Bejsovec, A., and Martinez Arias, A. (1991). Roles of wingless in patterning the larval epidermis of *Drosophila*. *Development* 113, 471–485.
- Bejsovec, A., and Wieschaus, E. (1995). Signaling activities of the *Drosophila* wingless gene are separately mutable and appear to be transduced at the cell surface. *Genetics* 139, 309–320.
- Bergeron, J.J., Di Guglielmo, G.M., Baass, P.C., Authier, F., and Posner, B.I. (1995). Endosomes, receptor tyrosine kinase internalization and signal transduction. *Biosci. Rep.* 15, 411–418.
- Bohm, S.K., Grady, E.F., and Bunnnett, N.W. (1997). Regulatory mechanisms that modulate signaling by G-protein-coupled receptors. *Biochem. J.* 322, 1–18.
- Cadigan, K.M., Fish, M.P., Rulifson, E.J., and Nusse, R. (1998). Wingless repression of *Drosophila* frizzled 2 expression shapes the Wingless morphogen gradient in the wing. *Cell* 93, 767–777.
- Carpenter, G. (2000). The EGF receptor: a nexus for trafficking and signaling. *Bioessays* 22, 697–707.
- Ceresa, B., and Schmid, S. (2000). Regulation of signal transduction by endocytosis. *Curr. Opin. Cell Biol.* 12, 204–210.
- Clifford, R., and Schupbach, T. (1992). The torpedo (DER) receptor tyrosine kinase is required at multiple times during *Drosophila* embryogenesis. *Development* 115, 853–872.

- Connolly, C.N., Futter, C.E., Gibson, A., Hopkins, C.R., and Cutler, D.F. (1994). Transport into and out of the Golgi complex studied by transfecting cells with cDNAs encoding horseradish peroxidase. *J. Cell Biol.* **127**, 641–652.
- Denef, N., Neubuser, D., Perez, L., and Cohen, S.M. (2000). Hedgehog induces opposite changes in turnover and subcellular localization of patched and smoothened. *Cell* **102**, 521–531.
- Dickinson, W.J., and Thatcher, J.W. (1997). Morphogenesis of denticles and hairs in *Drosophila* embryos: involvement of actin-associated proteins that also affect adult structures. *Cell Motil. Cytoskeleton* **38**, 9–21.
- Entchev, E.V., Schwabedissen, A., and Gonzalez-Gaitan, M. (2000). Gradient formation of the TGF- β homolog Dpp. *Cell* **103**, 981–991.
- Freeman, M. (2000). Feedback control of intercellular signaling in development. *Nature* **408**, 313–319.
- Gabay, L., Scholz, H., Golembo, M., Klaes, A., Shilo, B.Z., and Klambt, C. (1996). EGF receptor signaling induces pointed P1 transcription and inactivates Yan protein in the *Drosophila* embryonic ventral ectoderm. *Development* **122**, 3355–3362.
- Gonzalez, F., Swales, L., Bejsovec, A., Skaer, H., and Martinez Arias, A. (1991). Secretion and movement of wingless protein in the epidermis of the *Drosophila* embryo. *Mech. Dev.* **35**, 43–54.
- Incardona, J.P., Lee, J.H., Robertson, C.P., Enga, K., Kapur, R.P., and Roelink, H. (2000). Receptor-mediated endocytosis of soluble and membrane-tethered Sonic hedgehog by Patched-1. *Proc. Natl. Acad. Sci. USA* **97**, 12044–12049.
- Kirchhausen, T. (1999). Adaptors for clathrin-mediated traffic. *Annu. Rev. Cell. Dev. Biol.* **15**, 705–732.
- Kurz, D.J., Decary, S., Hong, Y., and Erusalimsky, J.D. (2000). Senescence-associated (beta)-galactosidase reflects an increase in lysosomal mass during replicative ageing of human endothelial cells. *J. Cell Sci.* **113**, 3613–3622.
- Lawrence, P.A., Sanson, B., and Vincent, J.P. (1996). Compartments, wingless and engrailed: patterning the ventral epidermis of *Drosophila* embryos. *Development* **122**, 4095–4103.
- Lecourtois, M., Alexandre, C., Dubois, L., and Vincent, J.-P. (2001). Wingless capture by Frizzled and Frizzled2 in *Drosophila* embryos. *Dev. Biol.*, in press.
- Levkowitz, G., Waterman, H., Ettenberg, S.A., Katz, M., Tsygankov, A.Y., Alroy, I., Lavi, S., Iwai, K., Reiss, Y., Ciechanover, A., et al. (1999). Ubiquitin ligase activity and tyrosine phosphorylation underlie suppression of growth factor signaling by c-Cbl/Sli-1. *Mol. Cell* **4**, 1029–1040.
- Leyns, L., Bouwmeester, T., Kim, S.H., Piccolo, S., and De Robertis, E.M. (1997). Frzb-1 is a secreted antagonist of Wnt signaling expressed in the Spemann organizer. *Cell* **88**, 747–756.
- Lin, X., and Perrimon, N. (1999). Dally cooperates with *Drosophila* Frizzled 2 to transduce Wingless signaling. *Nature* **400**, 281–284.
- Martinez Arias, A. (1993). Development and patterning of the larval epidermis of *Drosophila*. In *The Development of Drosophila melanogaster*, M. Bate and A. Martinez Arias, eds. (Cold Spring Harbor, NY: Cold Spring Harbor Laboratory Press), pp. 517–608.
- Moline, M.M., Southern, C., and Bejsovec, A. (1999). Directionality of Wingless protein transport influences epidermal patterning in the *Drosophila* embryo. *Development* **126**, 4375–4384.
- Payre, F., Vincent, A., and Carreno, S. (1999). ovo/svb integrates Wingless and DER pathways to control epidermis differentiation. *Nature* **400**, 271–275.
- Pfeiffer, S., Alexandre, C., Calleja, M., and Vincent, J.P. (2000). The progeny of wingless-expressing cells deliver the signal at a distance in *Drosophila* embryos. *Curr. Biol.* **10**, 321–324.
- Reinke, R., and Zipursky, S.L. (1988). Cell-cell interaction in the *Drosophila* retina: the bride of sevenless gene is required in photoreceptor cell R8 for R7 cell development. *Cell* **55**, 321–330.
- Sanson, B., White, P., and Vincent, J.P. (1996). Uncoupling cadherin-based adhesion from wingless signaling in *Drosophila*. *Nature* **383**, 627–630.
- Sanson, B., Alexandre, C., Fascetti, N., and Vincent, J.P. (1999). Engrailed and hedgehog make the range of Wingless asymmetric in *Drosophila* embryos. *Cell* **98**, 207–216.
- Schweitzer, R., Howes, R., Smith, R., Shilo, B.Z., and Freeman, M. (1995a). Inhibition of *Drosophila* EGF receptor activation by the secreted protein Argos. *Nature* **376**, 699–702.
- Schweitzer, R., Shaharabany, M., Seger, R., and Shilo, B.Z. (1995b). Secreted Spitz triggers the DER signaling pathway and is a limiting component in embryonic ventral ectoderm determination. *Genes Dev.* **9**, 1518–1529.
- Sevrioukov, E.A., He, J.P., Moghrabi, N., Sunio, A., and Kramer, H. (1999). A role for the deep orange and carnation eye color genes in lysosomal delivery in *Drosophila*. *Mol. Cell* **4**, 479–486.
- Strigini, M., and Cohen, S.M. (2000). Wingless gradient formation in the *Drosophila* wing. *Curr. Biol.* **10**, 293–300.
- Sunio, A., Metcalf, A.B., and Kramer, H. (1999). Genetic dissection of endocytic trafficking in *Drosophila* using a horseradish peroxidase-bridge of sevenless chimera: hook is required for normal maturation of multivesicular endosomes. *Mol. Biol. Cell* **10**, 847–859.
- Teleman, A.A., and Cohen, S.M. (2000). Dpp gradient formation in the *Drosophila* wing imaginal disc. *Cell* **103**, 971–980.
- Tsao, P., and Zastrow, M. (2000). Downregulation of G protein-coupled receptors. *Curr. Opin. Neurobiol.* **10**, 365–369.
- Tsuda, M., Kamimura, K., Nakato, H., Archer, M., Staatz, W., Fox, B., Humphrey, M., Olson, S., Futch, T., Kaluza, V., et al. (1999). The cell-surface proteoglycan Dally regulates Wingless signaling in *Drosophila*. *Nature* **400**, 276–280.
- van den Heuvel, M., Nusse, R., Johnston, P., and Lawrence, P.A. (1989). Distribution of the wingless gene product in *Drosophila* embryos: a protein involved in cell-cell communication. *Cell* **59**, 739–749.
- Van Vactor, D.L., Cagan, R.L., Kramer, H., and Zipursky, S.L. (1991). Induction in the developing compound eye of *Drosophila*: multiple mechanisms restrict R7 induction to a single retinal precursor cell. *Cell* **67**, 1145–1155.
- Vincent, J.P., and O'Farrell, P.H. (1992). The state of engrailed expression is not clonally transmitted during early *Drosophila* development. *Cell* **68**, 923–931.
- Wang, S., Krinks, M., Lin, K., Luyten, F.P., and Moos, M. (1997). Frzb, a secreted protein expressed in the Spemann organizer, binds and inhibits Wnt-8. *Cell* **88**, 757–766.
- Wasserman, J.D., Urban, S., and Freeman, M. (2000). A family of rhomboid-like genes: *Drosophila* rhomboid-1 and roughoid/rhomboid-3 cooperate to activate EGF receptor signaling. *Genes Dev.* **14**, 1651–1663.
- Wasylyk, C., Bradford, A.P., Gutierrez-Hartmann, A., and Wasylyk, B. (1997). Conserved mechanisms of Ras regulation of evolutionary related transcription factors, Ets1 and Pointed P2. *Oncogene* **14**, 899–913.
- Zecca, M., Basler, K., and Struhl, G. (1996). Direct and long-range action of a wingless morphogen gradient. *Cell* **87**, 833–844.
- Zhang, J., and Carthew, R.W. (1998). Interactions between Wingless and Dfz2 during *Drosophila* wing development. *Development* **125**, 3075–3085.
- Zimmerman, L.B., De Jesus-Escobar, J.M., and Harland, R.M. (1996). The Spemann organizer signal noggin binds and inactivates bone morphogenetic protein 4. *Cell* **86**, 599–606.